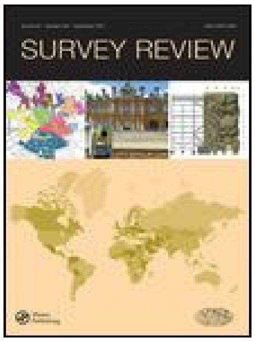

Taylor & Francis
Taylor & Francis Group

Survey Review

ISSN: 0039-6265 (Print) 1752-2706 (Online) Journal homepage: http://www.tandfonline.com/loi/ysre20

Extraction of Urban 3D Features from Lidar Data Fused with Aerial Images Using an Improved Mean Shift Algorithm

Chun Liu, Hangbin Wu & Yunling Zhang

Survey Review, **43**, 322, pp. 402-414 (September 2011)

EXTRACTION OF URBAN 3D FEATURES FROM LIDAR DATA FUSED WITH AERIAL IMAGES USING AN IMPROVED MEAN SHIFT ALGORITHM

Chun Liu[1,2], Hangbin Wu[1], and Yunling Zhang[1,3]

[1] Department of Survey and Geo-Informatics, Tongji University, Shanghai, China, 200092
[2] Key Laboratory of Advanced Engineering Surveying of SBSM, Shanghai, China, 200092
[3] China Highway Engineering Consulting Group Company Ltd. Beijing, China, 100097

ABSTRACT

An approach is proposed for the extraction of the urban three-dimensional features efficiently and accurately. In this method, firstly, both the LIDAR data and the aerial images are respectively pre-processed and matched using the affine transformation model .In order to exploit the spectral data and classify the LIDAR data with high accuracy, a data extraction procedure is employed which extracts the converted pixel values of the aerial image to LIDAR data. Then, an improved Mean Shift algorithm is employed to classify the LIDAR data fused with reflected intensity and spectrum attribute into groups by kinds of feature, such as buildings, vegetation, water etc. The classification accuracy is evaluated by space accuracy and confusion matrix evaluation. Finally, the 3D models of interested regions are quickly constructed based on the classified points and the aerial-image by SketchUp. Using this method, the 3D models of urban objects could be easily extracted and constructed.

KEYWORDS: LIDAR, Data Fusion, 3D Urban Modelling, Aerial Imagery

INTRODUCTION

LIDAR (Light Detection and Ranging) is an active remote sensing system, which utilizes a laser beam for detection and measurement to provide three-dimensional information of the earth's surface and objects. Due to its capability, there are wide applications for LIDAR data, such as 3D city models, urban planning, design of telecommunication networks, vegetation monitoring and disaster management. By contrast with traditional photogrammetry, the 3D urban data captured using LIDAR is of higher speed, better vertical accuracy and lower cost **[9]**.

Since the 1990s, automated or semi-automated reconstruction of urban buildings from photographs has been widely developed and deeply studied **[4], [11]**. Due to the complexity of the technology and the objects, model reconstruction with LIDAR data has been continuously tried and has achieved some results. However, it has suffered from some problems **[6]**. More recently, LIDAR or SAR has become a research focus using feature extraction by integration of multispectral/hyperspectral images, **[16]**.

However, automatic interpretation based on image classification is a concrete application of pattern recognition and artificial intelligence in remote sensing technology. Usually, classification by pattern recognition can be divided into two methods: supervised classification and unsupervised classification. Supervised classification is based on the principle that uncertain pixels can be identified with determined pixels, and the common supervised classification methods are Maximum Likelihood Classifier (MLC), Bayesian Method and K-Neighbourhood Method.

Contact: C Liu. e-mail: liuchun@tongji.edu.cn

DOI 10.1179/003962611X13055561708821

Artificial intelligent classification method calls for understanding the image structure or texture information first, and then the image can be classified. It mainly includes the artificial neural network method **[8]**, fuzzy mathematic method **[18]**, fuzzy neural model and expert system method **[2]**. Among those approaches, the artificial neural network method has been introduced into remote sensing image classification and obtained good results. However, there are two apparent disadvantages in the neural network method: (1) the selection of the network structure and parameters has not enough theoretical basis; and (2) the classification results are highly dependent on experiential elements because of over-learning and local minimum point defects.

Interpretation based on spectral information is not applicable in interpreting and classifying the aerial-images due to the lack of spectral information. The diversity of real objects and their spatial distributions create complex phenomena, including the same material having different spectral properties, the different materials with similar spectral properties, and mixed pixels, all of which mean that the results of unsupervised classifications can be very poor. Therefore, the most popular method of extracting water features from aerial images is by artificial interpretation or supervised classification. However, with the effects of atmosphere, environment and classification samples, supervised classification can often lead to misclassifications. The primary goal of this paper is to present a new water feature extraction method based on aerial images fused with airborne LIDAR data. By introducing point cloud data from LIDAR as a supplement, the approach takes full advantages of wave bands available both in the LIDAR systems and the water spectrum in particular bands. Through fusing the spatial information of LIDAR point cloud data with colour information of aerial image, water feature extraction can be carried out more precisely

Feature extraction from LIDAR data mostly uses the geometric characteristics. As a result, while buildings are successfully extracted and reconstructed, the irregular shape of some features such as vegetation cannot be preserved **[14]**. However, vegetation is one of the key issues in urban environment planning and monitoring **[5]**.

Considering the geometric limitation of LIDAR, in the research for this paper, classification was applied before feature extraction. The classification processing for LIDAR data could be helpful in improving the reliability and accuracy of extraction. Moreover, it can assign the point in a point cloud to a certain group, thus the interested features will be paid more attention, and the efficiency could be increased.

In LIDAR data, a lot of objects' points are close together in location and similar in elevation, such as roads and grass, buildings and trees. For those points, problems will be encountered using traditional classification methods **[17]**. Generally, the material of these objects is different and, normally, the spectral information in images is also different and can be easily used for detection and reorganization. Thus, in this paper, the spectral data of an aerial image is exploited and extracted to the LIDAR data to achieve much improved classification results.

The main algorithm used in this paper is Mean Shift, which is popularly used in image segmentation and object detection **[3]**. With the help of spectral data and the intensity data, the kernel function of the Mean Shift algorithm is extended and made suitable for multi-dimensional data classification. Therefore, both building and vegetation features can be respectively at the same time.

OBJECTIVE AND METHODOLOGY

The 3D feature extraction is divided into three stages: pre-processing, classification and feature extraction, and Figure 1 describes the methodology used, which is explained as follows:

1. Pre-processing of the point cloud. During pre-processing, height smoothing, geo-registration and information extraction are introduced into the point cloud and aerial image in sequence. Due to the obviously influence of any gross error point, height smoothing is firstly used to eliminate any gross errors in the raw LIDAR data by setting the height threshold and radius of a search window. This is helpful in reducing the probability of misclassification. Then, in order to exploit the spectral data, the registration employs the affine transformation model by manually selecting several homologous points to make ensure the two data sets are in the same coordinate system. This enables the spectral values to be extracted from the matched image to the LIDAR data.

As spacial data is insufficient for classification and spectral data is helpful for recognizing the object, more and more researchers use spectral data from all kinds of images to fuse with LIDAR data. During pre-processing, the employed colour space of spectrum are transferred from RGB space to L*a*b* space. To obtain a meaningful classification, perceived colour differences should correspond to Euclidean distances in the colour space chosen to represent the features. L*a*b* space was especially designed to best approximate perceptually uniform colour spaces. The dependence of all three coordinates on the traditional RGB colour values is nonlinear.

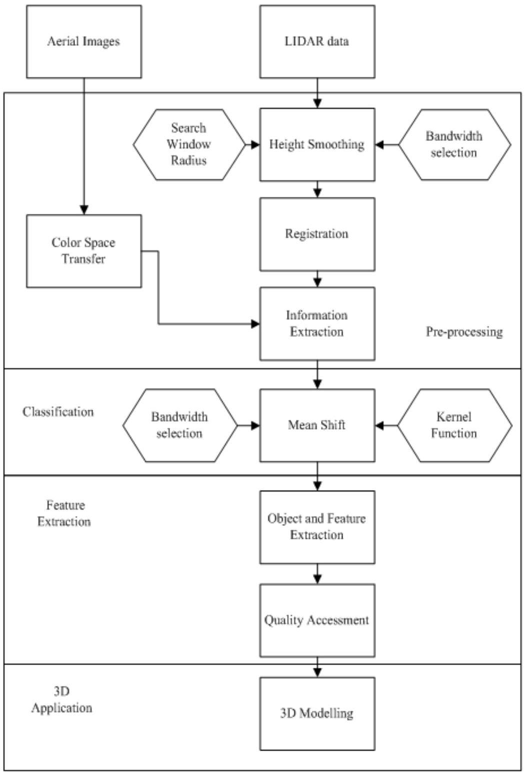

Fig. 1. Operation Flowchart

A computational module based on the Mean Shift algorithm is an extremely versatile tool for feature space analysis and can provide reliable solutions for many tasks **[17]**. Thus, this algorithm is introduced to classify the point clouds in the experiment. In addition, the key attribute of the Mean Shift algorithm is an appropriate kernel function for bandwidth setting and selection.

When an appropriate classification is applied to the point cloud, the ground features can be extracted through an analysis of the result of classification. In the end, a 3D scene can be quickly modelled based on the extracted features using SketchUp.

STUDY AREA

The data used in this paper was produced by the Woolpert Company for the Ohio Imagery Data Project. The data can be downloaded from:

http://metadataexplorer. gis.state.oh.us/metadataexplorer/explorer.jsp.

It was captured by a Leica ALS digital LIDAR system during March to May 2006. In this experiment, a small part of the data was used which includes an aerial image and a point cloud set. The point cloud includes 3,569 points and mainly stores vegetation, bare soil, buildings, and roads. The area of the research region is about 0.016 square kilometres. The aerial image is 365 pixels by 482 pixels and every pixel equates to about 0.3 m. The LIDAR data and the aerial image are shown in Figure 2.

a Aerial image data

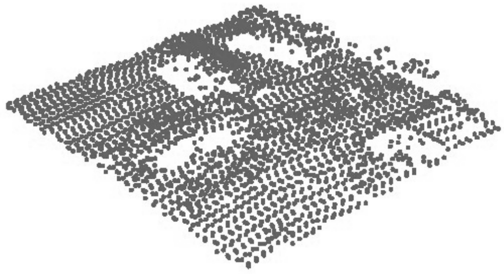

b LIDAR point cloud

Fig. 2. Experimental data in the study area

PRE-PROCESSING

Data Smoothing

Data smoothing is firstly used to detect the gross error points in the point cloud. By establishing a search window for each point, whether the point is a gross error is determined by comparing the height difference with other points in the search area.

The principle of data smoothing is described in Figure 3. The key parameters for data smoothing are height difference threshold and the search window radius. In this paper, the height difference threshold is taken as the average height plus 3 times the standard deviation of heights in the search window, and the radius of the search window is taken as 3 times the average distance of the sample data.

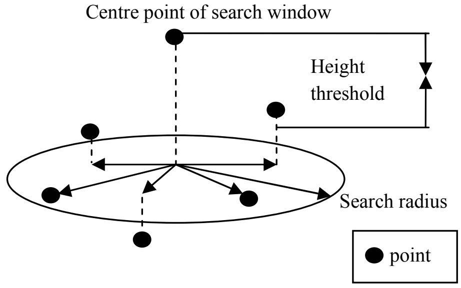

Fig. 3. Principle of Height smooth

Geometric registration

The point cloud has three-dimensional position information of high accuracy, while normal aerial images do not contain geometric coordinate information. Before the two types of data can be joined for feature extraction, registering to a single coordinate system must be completed. Fourteen homologous points were selected in the aerial image and the point cloud. The affine transformation based on six parameters of the Plane Coordinate Transformation Model was applied to complete registration. The model is given in Eq. (1).

$$\begin{aligned} x' &= Ax + By + C \\ y' &= Dx + Ey + F \end{aligned} \tag{1}$$

Where (x', y') represents the pixel position of the homologous point in the aerial image, and (x, y) represents the point position from the LIDAR data. The least squares solution of six parameters is obtained in Table 1 through the fourteen homologous points. The residual error of registration is about 5 pixels. In this experiment, the accuracy of registration is sufficient for further use.

Table 1. *Coordinate transfer parameters*

Parameters	A	B	C	D	E	F
Value	0.6676065	0.000883	-0.000711	-0.669068	620313.6	4166486.8

Colour Space Transfer

As introduced above, colour information is important in object detection, such as roads, grass, buildings or trees. The selection of colour space is also vital when using the pixel values of an image. Through experiment, we found that the L*a*b* space is adaptive and more suitable than RGB space for classification using the Mean Shift algorithm. So, before advanced processing, the pixel values of the aerial image were converted from RGB space to L*a*b* space.

A readily accessible conversion equation is as follows: firstly, RGB coordinates should be transferred to CIE-XYZ coordinates using the following metric. Let *R, G* and *B* be the pixel values in RGB space of a certain pixel of image, *X, Y* and *Z* are the pixel values in CIE-XYZ space. The equation of transformation is given as Eq. (2).

$$\begin{bmatrix} (X) \\ (Y) \\ (Z) \end{bmatrix} = \begin{bmatrix} 0.412453 & 0.35758 & 0.180423 \\ 0.212671 & 0.71516 & 0.072169 \\ 0.019334 & 0.11919 & 0.950227 \end{bmatrix} \begin{bmatrix} R \\ G \\ B \end{bmatrix} \tag{2}$$

The relationship between L*a*b* and CIE-XYZ is illustrated in Eq. (3) and (4) using the *X, Y, Z* data captured by equation (2). In the equation, *Xn, Yn, Zn* represent the value of lights stimulus under the CIE standard lighting conditions. In general, *Xn=95.05, Yn=100, Zn=108.89*, when *X/Xn>0.008856, Y/Yn>0.008856, Z/Zn>0.008856*. Eq. (3) is suitable for conversion.

$$\begin{aligned} L^* &= 116\,(Y/Y_n)^{1/3} - 16 \\ a^* &= 500\,[(X/X_n)^{1/3} - (Y - Y_n)^{1/3}] \\ b^* &= 200\,[(Y/Y_n)^{1/3} - (Z - Z_n)^{1/3}] \end{aligned} \tag{3}$$

Otherwise, when *X/Xn<0.008856 Y/Yn<0.008856 or Z/Zn<0.008856*, another expression represents the relationship (Eq. 4).

$$\begin{aligned} L^* &= 903.3[7.787\,(Y/Y_n)^{1/3} + 16/116] \\ a^* &= 500[(X/X_n)^{1/3} - (Y - Y_n)^{1/3}] \\ b^* &= 200[(Y/Y_n)^{1/3} - (Z - Z_n)^{1/3}] \end{aligned} \tag{4}$$

Data fusion

As the aerial image and the point cloud have now been geo-registered, the two data sets can be displayed in the same coordinate system and, for each point, we can easily find its corresponding pixel in the aerial image. Then the spectral information is extracted from the aerial image to the LIDAR data through an overlay operation.

Point Cloud Classification with Mean Shift

Mean Shift Principle

Mean Shift is a simple iterative procedure that shifts each data point to the average of data points by neighbourhood search and calculation. Mean Shift based feature extraction from LIDAR data is an extension of image segmentation. Each pixel associates with a significant mode of the joint domain density located in its neighbourhood **[3]**.

Let data be a finite set *S* embedded in the *n*-dimensional Euclidean Space, *X*. Let *K* be a kernel function and *w(s)* a weight function. The mean with kernel function *K* and bandwidth matrix *H* at a certain point $x \in X$ is defined as:

$$m(x) = \frac{\sum_{s \in S} K_H(s-x)w(s)s}{\sum_{s \in S} K_H(s-x)w(s)} \tag{5}$$

where

$$K_H = |H|^{-1/2} K(H^{-1/2}x) \tag{6}$$

The evolution of X in the form of iterations $X \leftarrow m(X)$ with $m(X) = \{m(x); x \in X\}$ is called the Mean Shift algorithm. As the gradient direction of probability density is in accordance with the direction that probability density increases fastest, the direction of Mean Shift vector $m(x) - x$ is generally toward the region with densest points, as Figure 4 illustrated.

For each point $x \in X$, there is a sequence $x, m(x), m(m(x)), \cdots$ after the Mean Shift iteration starts. The location of the sequence is regarded as the trajectory of *x*. When $\|m(x) - x\| < \varepsilon$, the iteration stops, where ε is a minimum value.

Otherwise, in practice, the bandwidth matrix H is chosen either as diagonal $H = diag[h_1^2, \cdots, h_d^2]$, or proportional to identity matrix $H = h^2 I$, so that only the bandwidth parameter $h > 0$ must be provided **[3]**. The weight *w(s)* can be fixed throughout the processing or re-evaluated after each iteration.

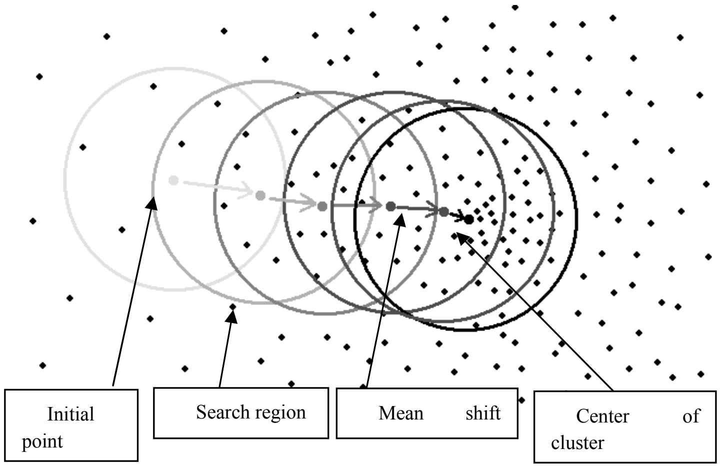

Fig. 4. Trajectory of a point finding centre of cluster

As Figure 5 shows, in a non-uniform data set, for several iterations, each of the 34 non-uniform distributed points are convergent to its cluster centre point separately. Then, they can be classified into three clusters.

Kernel Function Set

The kernel function is a kind of weight function used in nonparametric function estimation. It gives the weights of the nearby points in making an estimate. Kernel functions are piecewise continuous, bounded, symmetric around zero, concave at zero, real valued, and for convenience often integrate to one. They can be probability density functions. Usually, the kernel functions are defined under the domain *[-1, 1]*.

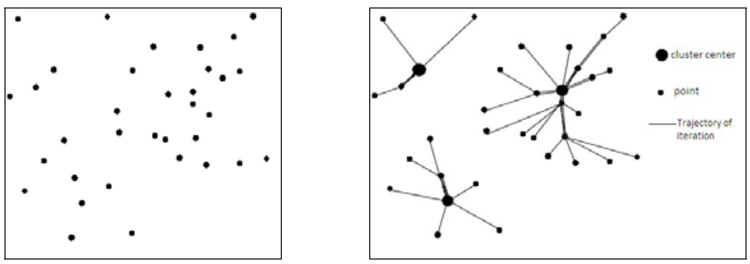

a. Non-uniform distributed Data Set b. Trajectories of Mean Shift cluster process

Fig. 5. Mean Shift cluster process

Definition: Let X be the n-dimensional Euclidean space, Rn. Denote the i^{th} component of $x \in X$ by x_i. The norm of $x \in X$ is a non-negative number $\|x\|$ such that $\|x\|^2 = \sum_{i=1}^{n} |x_i|^2$. The inner product of x and y in X is $\langle x, y \rangle = \sum_{i=1}^{n} x_i y_i$. A function $K : X \to R$ is regarded as a kernel if there exists a profile, $k : [0, \infty] \to R$, such that:

$$K(x) = k(\|x\|^2) \tag{7}$$

and

1) k is non-negative.
2) k is not increasing: $k(a) \geq k(b)$ if $a<b$
3) k is piecewise continuous and $\int_0^\infty k(r)dr < \infty$

Otherwise, if K and H are kernels, then $K+H$ is also a kernel defined as:

$$(K + H)(x) = K(x) + H(x) \tag{8}$$

And KH is a kernel defined as:

$$KH(x) = K(x) \times H(x) \tag{9}$$

The following kernel functions are popularly used, as illustrated in Table 2.

Table 2. *Commonly used kernel functions*

Kernel function	Definition	Figure
Uniform	$K(x) = \begin{cases} 1 & if \ \|x\| < 1 \\ 0 & if \ \|x\| \geq 1 \end{cases}$	
Epanechnikov	$K(x) = \begin{cases} 1 - \|x\|^2 & if \ \|x\| < 1 \\ 0 & if \ \|x\| \geq 1 \end{cases}$	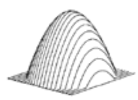
Gaussian	$K(x) = e^{-\|x\|^2}$	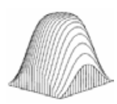

In this paper, considering the rate of convergence and the sensibility of features, Epanechnikov is chosen as the basic kernel function.

Meanwhile, in the fused data *(x, y, z, l, a, b, i),* space coordinate *(x, y, z),* chromaticity coordinate *(l, a, b)* and reflectivity intensity *(i)* belong to separate independent Euclidean spaces. Therefore, according to Eq. (6) and (8), the multi-variate kernel is defined as the product of three radial symmetric kernels, and the Euclidean metric allows a single bandwidth parameter for each domain (Eq. 10).

$$K(x) = \frac{C}{h_s^3 h_c^3 h_r} k\left(\left\|\frac{x_s}{h_s}\right\|^2\right) k\left(\left\|\frac{x_c}{h_c}\right\|^2\right) k\left(\left\|\frac{x_r}{h_r}\right\|^2\right) \tag{10}$$

Where x_s means space coordinate *(x, y, z)*, x_c is the chromaticity coordinate *(l, a, b)*, and x_r is the reflectivity intensity *(i)*; h_s, h_c, h_r means corresponding bandwidth for each domain. *C* is a constant.

Weight Selection

Weight function *w(s)* is an important component of the Mean Shift algorithm. It can be used to determine the contribution when using a certain sample point or a kind of dataset to calculate the Mean Shift vector. In multi-dimensional data applications, weight function is normally used to separate the contribution from different kinds of datasets when calculating the new Mean Shift vector centre.

In this paper, in order to have a comparison and obtain the best effect when classifying the LIDAR data, a series of weights are added to the different dimensional fused LIDAR data. From the experiment, we know that:

1 - when setting an equal weight for space domain *(x,y,z)* and reducing the weight for other domain to 0, the feature with the largest height difference from surroundings can be extracted, such as tall trees, roofs etc. But the extraction accuracy of grass is not as good.

2 - considering that a grass point and the road point are close in elevation; they cannot be distinguished using only the space domain. However, grass and road are composed of different materials and obviously with different reflectivity characteristics. Thus, the intensity domain *(i)* was added to the experiment. When increasing the weight of intensity domain *(i)* to 5, the road and grass are classified well.

3 - in order to distinguish between a low building and road, the chromaticity data was used in experiment. When changing the weight for *(l,a,b)*, we get the conclusion that the *(a, b)* vector plays a more important role than *(l)*.

Bandwidth Selection

Bandwidth is the most important parameter in the Mean Shift algorithm. It decides the number of points used to calculate the new Mean Shift vector. It is also the threshold to determine whether the point set belongs to group A or group B.

In this experiment, bandwidth was reduced from 0.4 to 0.1 by manual intervention. Combined with the weight function, we use space, chromaticity and intensity data to start the experiment. The optimal bandwidths for case data are $h_s = 0.2$, $h_c = 0.2$ and $h_i = 0.1$.

Feature Extraction

Based on the obtained 3D mesh, normal vector was calculated for each mesh triangle as the geometric indicator of the 3D mesh of Lidar data, and 3D construction is also conducted. By considering the normal vector of the 3D mesh, the gradient of the neighbouring triangle is calculated to determine the feature points among the point cloud, and some line segment can be obtained by connecting these feature points.

Quality Assessment

Quality assessment was conducted from two aspects: detail analysis and statistical ensemble. On the one hand, a building edge was manually digitized in the aerial image as the ground truth. Then, to assess the clustering quality, the cluster edge points were contrasted to the ground truth line.

The distances between ground truth line and cluster edge points were calculated and the statistics analysed. The error distribution can be seen in Figure 8. The maximum difference was 3.419m.

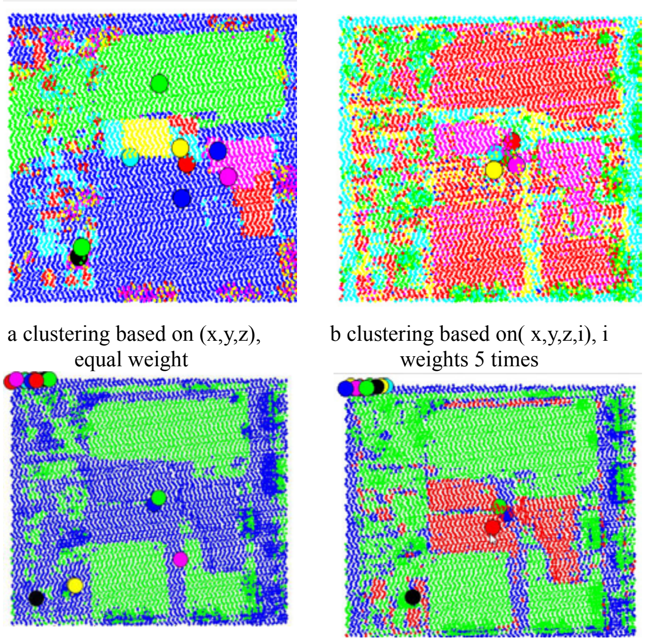

a clustering based on (x,y,z), equal weight

b clustering based on(x,y,z,i), i weights 5 times

c clustering based on (x,y,z,l,a,b), equal weight

d clustering based on (x,y,z,l,a,b), a,b weights 3 times

Fig. 6. Weight influence on clustering

On the other hand, the assessment of classification accuracy can be determined by a confusion metric, shown in Table 3. The general accuracy of classification can achieve 85.64%, which is a good result of classification.

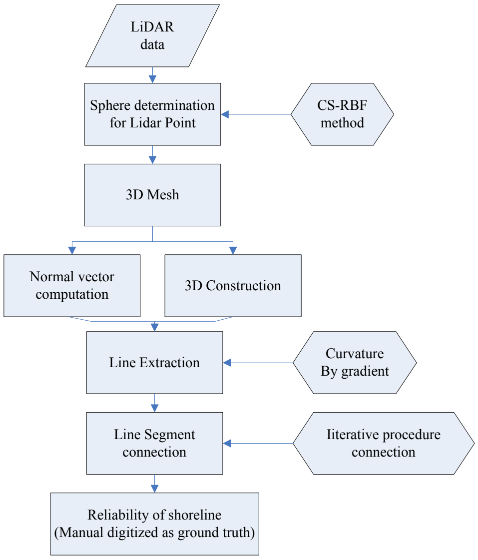

Fig. 7. Methodology of the 3D line extraction

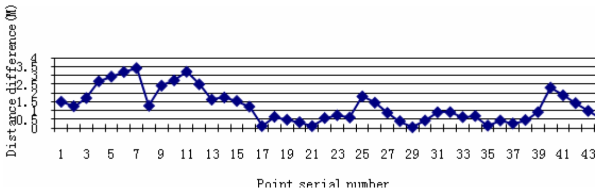

Fig. 8. Distance difference between Ground truth line and cluster edge points

Table 3. *Confusion metric of classification*

Number of points		Reference cluster			Total	User accuracy
		building	trees	land		
Practical cluster	building	5582	28	36	5646	98.87%
	trees	288	21524	862	22674	95.06%
	land	1988	5710	26833	34531	77.63%
Total		7858	27262	27731	62708	
Mapping accuracy		71.04%	78.95%	96.86%		
Omission errors		28.96%	21.05%	3.14%		
Commission errors		0.81%	4.22%	28.31%		
General accuracy					85.64%	

3D MODELLING APPLICATION

With a small amount of manual checking of the classification, any misclassification mainly caused by the cars, can be corrected. Then, the accurately classified points representing the ground feature can be the foundation of 3D modelling.

Firstly, the DEM of the study area can be extracted from the land point cluster and exported to SketchUp. The aerial images can be used as the texture of the DEM surface, for the next step of modelling 3D buildings and trees.

Then, the building point cluster is imported to the SketchUp as a layer (see Figure 9), the 3D buildings can be used to construct models, with help of the points and the aerial images information.

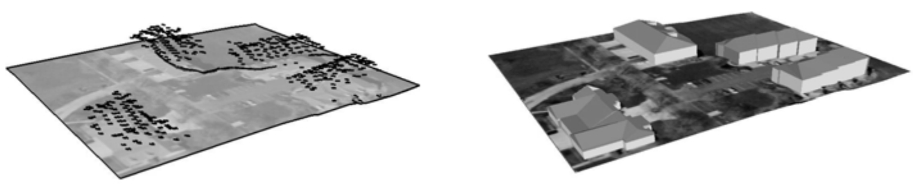

a. Imported building points b.3D buildings modelling

Fig. 9. Procedure of buildings modelling

Similarly, the trees point cluster is used to establish the 3D trees, as shown in Figure 10. The single tree model can be found in SketchUp Material Database from the Internet.

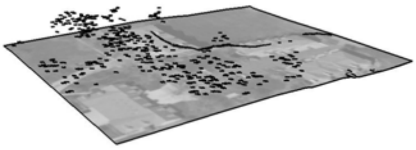

a. Imported trees points

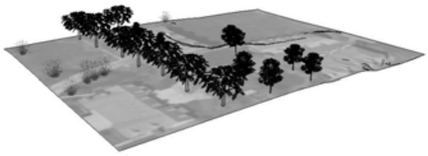

b. 3D trees modelling

Fig. 10. Procedure of trees modelling

In the end, all the layers are combined, and then the ground features can be reconstructed in Figure 11.

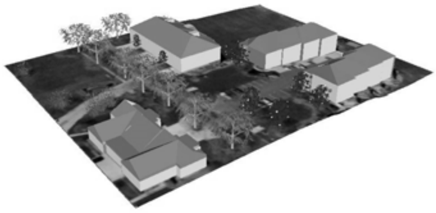

Fig. 11 Final model

CONCLUSION

This paper proposes a method of obtaining 3D models from LIDAR data and aerial images, which has been proved feasible in the experiment. The key issues in this paper are: 1) LIDAR data registration with aerial images; 2) classification using the Mean Shift algorithm; and finally 3) reconstruction of ground features. The image data plays two important roles. Firstly, the image is a data source in classification processing after geo-registration with LIDAR. Then, in 3D modelling, the image data are used as the texture for the DEM.

Simultaneously, the Mean Shift algorithm has been proved to be a feasible method to perform the point classification. Compared with other traditional classification methods, the Mean Shift algorithm is more suitable in multi-dimensional data classification. During the processing, bandwidth and weight function play an important role in point classification. It is worth noting that, the bandwidth is usually determined by manual intervention. The user may alter the bandwidth from large to small and then evaluate the results to choose the best value. In addition, a point cloud can help feature extraction and 3D modelling after its classification, which further extends the application fields of point cloud.

ACKNOWLEDGEMENTS

The work described in this paper was supported by Innovation Program of Shanghai Municipal Education Commission (Project ID:10ZZ25) and Key Laboratory of Geo-informatics of State Bureau of Surveying and Mapping (project ID:200914)

References

1. Barton, I. J. and Bathols J M., 1989. Monitoring floods with AVHRR[J].*Remote Sensing of Environment*.,30(1):89-94
2. Chen, X., Cai, X. and Li, H., 2007. Expert Classification Method Based on Patch-Based Neighborhood Searching Algorithm. *Geo-Spatial Information Science*. 10(1):37-43
3. Comaniciu, D., and Meer, P., 2002. Mean Shift: A robust approach toward feature space analysis. *IEEE Transactions on Pattern Analysis and Machine Intelligence,* 24 (5): 603-619
4. Debevec, P., et al., 1996. Modeling and Rendering Architecture from Photographs: A Hybrid Geometry and Image-Based Approach, In SIGGRAPH '96(August), 11-20
5. DeCandido, R., 2004. Recent changes in plant species diversity in urban Pelham Bay Park, 1947–1998. *Biological Conservation*, 120 (1):129-136
6. Haala, N., and Brenner, C., 1997. Generation of 3D City Models from Airborne Laser Scanning Data, *Proceedings EARSEL workshop on LIDAR remote sensing on land and sea*, :105- 112
7. Horwitz, H. M. and Nalepka, R.F., 1971. Estimating the Proportions of Objects within a Single Resolution Element of a Mulitispectral Scanner[J],*Proceeding of 7th International Symposium on Remote Sensing of Environment*.:pp 1307-1330.
8. Luo, J-C., Zhou, C-H. and Yang, Y., 2001. ANN Remote Sensing Classification Model and Its Integration Approach with Geoknowledge. *Journal of Remote Sensing*, 5(2):122-129
9. Mei, Z., et al., 2009. A Classification Method for Building Detection Based on LIDAR Point Clouds. *2009 Urban Remote Sensing Joint Event, Shang Hai*.
10. Munday, J. C. Jr. and Alföldi, T. T., 1979. LANDSAT test of diffuse reflectance models for aquatic suspended solids measurement. *Remote Sensing of Environment*,.8(2):169-183
11. Noronha, S., and Nevatia, R., 2001. Detection and Modeling of Buildings from Multiple Aerial Images. *IEEE Transactions on pattern analysis and machine intelligence,* 23 (5):501-518
12. Ohtake, Y., Belyaev, A., and Seidel, H-P., 2004. 3D Scattered Data Approximation with Adaptive Compactly Supported Radial Basis Functions]. Washington DC:*IEEE Computer Society*: 31-39
13. Ordoyne, C., 2008. Using MODIS data to characterize seasonal inundation patterns in the Florida Everglades. *Remote Sensing of Environment*. 112(11):4107-4119
14. Rutzinger, M., et al., 2006. Object-Based Building Detection based on Airborne Laser Scanning Data within GRASS GIS Environment. *Urban Data Management Symposium (Aalborg)*
15. Sabins, F. F., 1996. *Remote Sensing: Principles and Interpretations*. Third Edition W. H. Freeman
16. Tao, G., and Yasuoka, Y., 2002. Combining High Resolution Satellite Imagery and Airborne Laser Scanning Data for Generating Bareland DEM in Urban Areas. *International Archives of the Photogrammetry, Remote Sensing and Spatial Information Sciences,* 34 (5): W3
17. Wu, H., 2010. Classification and feature extraction of airborne LIDAR data fused with aerial image. Ph.D thesis. Tongji University
18. Zhao, Z.Y., Xu Y. M., 1996. The Foundation and Application of Fuzzy theory and neural network. Tsinghua University Press